

Large Area Deposition of $\mu\text{-Si}$ by Microwave PECVD

W.J. Soppe¹, C. Devilee¹, J. Löffler¹, A. Gajovic², P. Dubcek², D. Gracin², H.-J. Muffler¹
¹ECN-Solar Energy, P.O. Box 1, 1755 ZG Petten, The Netherlands, email: soppe@ecn.nl
²Rudjer Boskovic Institute, 1000 Zagreb, Bijenicka 54, Croatia

Abstract: Microwave PECVD has been applied to grow intrinsic microcrystalline ($\mu\text{-Si}$) and amorphous silicon (a-Si) layers for solar cell applications in a relatively low growth rate regime (0.1 - 0.3 nm/s). In this growth rate regime optically dense layers can be produced, which are entirely microcrystalline for silane fractions less than 5 % and which are amorphous for larger silane fractions. The best amorphous layers have an optical bandgap of about 1.6 eV and a structure factor R^* of about 0.1, Urbach energy E_U of about 55 meV and $\sigma_{\text{ph}}/\sigma_d$ in the range of 5×10^4 . Best microcrystalline layers, grown at a silane fraction of about 5 %, have an Urbach energy of 107 meV and $\sigma_{\text{ph}}/\sigma_d$ in the range of 5×10^2 .

Key Words: Microcrystalline Si, PECVD, Optical Properties.

1 Introduction

Application of $\mu\text{-Si}$ in thin film silicon solar cells offers a great perspective of achieving higher and more stable efficiencies of these devices than for a-Si devices, but this will only be accomplished in large-scale industrial production if the deposition rate of intrinsic $\mu\text{-Si}$ meets industrial demands [1,2].

Microwave PECVD is a deposition method that can fulfill these industrial demands. In previous papers [3,4] we have shown that the method is capable of deposition rates for $\mu\text{-Si}$ higher than 1 nm/s in a stationary mode. Furthermore, by the linear character of the microwave source, the method is inherently suitable for continuous processing (e.g. roll-to-roll production) on large areas. In order to combine high deposition rates and high material quality we have to optimize the deposition conditions. In a first optimization step intrinsic $\mu\text{-Si}$ of high quality is developed at low deposition rates r_d . The subsequent step is focused on a continuous increase of r_d without losses of film quality. This article presents the latest results of optical and structural properties of intrinsic $\mu\text{-Si}$ obtained by microwave PECVD.

2 Experimental Setup

2.1 Depositions by microwave PECVD

The depositions were carried out using a single chamber microwave PECVD reactor, in which a substrate holder with a substrate area of $60 \times 15 \text{ cm}^2$ moves underneath a linear microwave plasma source [3]. We varied the flow of silane while all other gas flows and deposition conditions were kept constant. The depositions took place simultaneously on glass substrates and on silicon wafers to allow various characterization techniques to be used on samples from the same batch.

Optical emission of the plasma (OES) was monitored in the wavelength range from 200-1000 nm, with a resolution of 0.6 nm. The optical emission of the transition H_α is monitored at 656 nm, and that of SiH^* is monitored at 412 nm.

2.2 Characterization of the silicon layers

Fourier Transform Photocurrent Spectroscopy (FTPS) was applied to obtain information on the defect density of the

layers. Dark conductivity was measured after evaporation of Al contacts on the layers, applying a constant voltage of 10 V between them. The photo conductivity was measured at a sun simulator (AM1.5, 25°C).

Reflection and transmission (R/T) spectra in the wavelength region between 330 and 1400 nm were obtained using an integrating sphere. The used monochromator has a resolution of 5 nm. To determine the hydrogen concentration c_H and the structure factor R^* , FTIR spectra in the range 400-4000 cm^{-1} were recorded by a Perkin-Elmer BX-II spectrometer (resolution of 8 cm^{-1}).

The optical constants (n, k) were obtained by analysis of the R/T spectra and curve fitting of the interference fringes in the IR transmission spectra [3].

3 Results

3.1 Plasma characteristics

The growth rates of the layers varied between 0.1 and 0.3 nm/s. Optical Emission Spectroscopy shows that the ratio of $H_\alpha/\text{SiH}^* > 1$ is obeyed for a deposition regime where the silane fraction is varied between 2 and 25 %. Thus, like in other PECVD systems this condition to grow microcrystalline silicon is fulfilled. The H_α/SiH^* ratio decreases linearly with

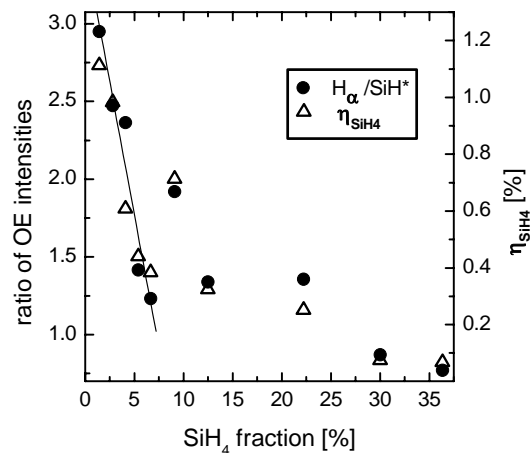


Figure 1 Ratio of optical emission (OE) intensities and silane utilization η_{SiH_4} against the silane fraction ($\Phi_{\text{SiH}_4}/(\Phi_{\text{SiH}_4} + \Phi_{\text{H}_2} + \Phi_{\text{Ar}})$).

increasing silane fractions in the range where it is lower than 8 %; this is indicated by a line in Fig. 1. At higher fractions a flattening of this decrease can be observed. The silane utilization η_{SiH_4} , defined as the growth rate divided by the SiH_4 flow ($\eta_{\text{SiH}_4} = r_d/\Phi_{\text{SiH}_4}$), shows the same behavior at increasing SiH_4 fractions (see Fig. 1). Therefore, these observations are an indication for a lower depletion of SiH_4 at higher SiH_4 flows.

3.2 Opto-electrical properties

Previous series of silicon layers deposited by microwave PECVD revealed relative high porosity as reflected by low refractive indices and high post-oxidation rates. This porosity appeared to be strongly correlated with the used silane fraction.

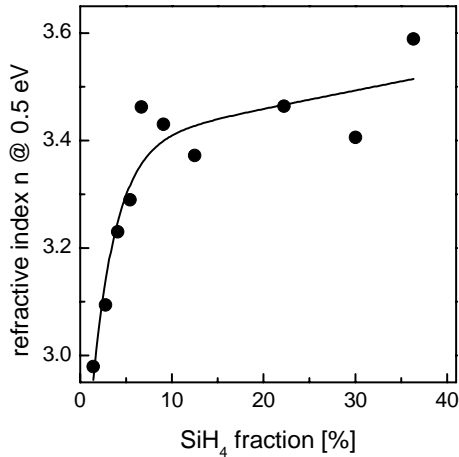


Figure 2 Refractive index n (0.5 eV) versus the silane fraction

In Figure 2, also a continuous decrease of the refractive index with decreasing silane fraction is demonstrated. But in this case, the mechanisms behind such a behavior are still to be resolved since the OES measurements give no indication of enhanced formation of sticky Si^* and SiH species at low (<5 %) silane fractions (i.e. low silane flows).

The structure factor R^* , as obtained from FTIR, can be correlated to the void density of amorphous Si layers. In Fig. 2 R^* shows a steep drop from almost 1.0 to about 0.1 if the silane fraction is increased from 1 to 6 % (see Fig. 3). In this regime the material changes from microcrystalline to amorphous. For silane fractions >10% the structure of the layers is not only determined by the silane flow during

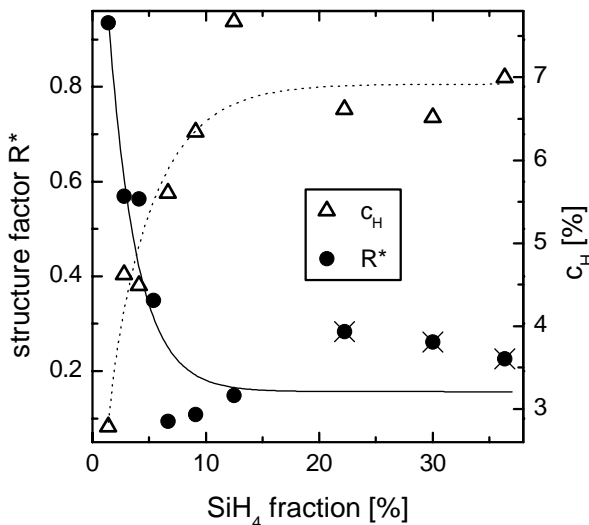


Figure 3 Structure factor R^* and hydrogen concentration c_H versus silane fraction

deposition, but also by the layer thickness. Thicker layers in this regime (in Fig. 3 marked with a cross) seem to have a higher void density and/or seem to start crystallization during growth, resulting in somewhat higher R^* . The hydrogen content in the layers increases with increasing silane fraction, from about 3 % in the entirely microcrystalline layers to about 8 % in the amorphous layers. These values are relatively low, but this can be attributed to the relatively high substrate temperature of 300 °C.

The dark conductivity (Fig. 4) shows a strong decrease with increasing silane fractions. This is the typical behavior that accompanies the transition from microcrystalline to amorphous structure. The photo conductivity remains more or less constant (about 10^{-5} S/cm) in this range of silane fractions so that the ratio of $\sigma_{\text{ph}}/\sigma_{\text{dark}}$ follows the inverse pattern of σ_{dark} . Thus, the transition can also be seen as a strong increase in $\sigma_{\text{ph}}/\sigma_{\text{dark}}$ with increasing silane fraction.

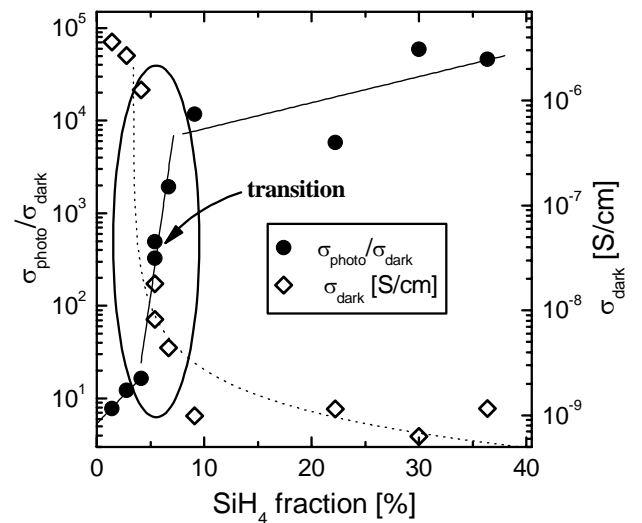


Figure 4 dependence of $\sigma_{\text{photo}}/\sigma_{\text{dark}}$ ratio and dark conductivity σ_{dark} on silane fraction

The Urbach tail energy E_U , as derived from FTPS measurements, is about 55 meV for the entirely amorphous layers (grown with silane fraction of 30 %) and 107 meV for microcrystalline layers grown in the $\mu\text{c-Si/a-Si}$ transition regime (silane fraction 5-8%).

Therefore, the opto-electrical properties indicate that these $\mu\text{c-Si}$ and a-Si layers are close to device quality material.

Acknowledgements

This work has been financially supported by the Dutch Ministry of Economic Affairs (Project No. TSIN3043) and by the European Commission under contract no. INCO-CT-2004-509178.

References

- [1] A.V. Shah et al, Progress in Photovoltaics, 12, 2004, 113-142.
- [2] K. Yamamoto, M. Yoshimi, Y. Tawada, Y. Okamoto, A. Nakjima, Sol. En. Mat. Sol. Cells 66 (2001) 117.
- [3] A.C.W. Biebericher, A.R. Burgers, C. Devilee and W.J. Soppe, Proceedings 19th European Photovoltaic Solar Energy Conference (2004) 1485.
- [4] W.J. Soppe, et al, Presented at the 20th European Photovoltaic Solar Energy Conference, Barcelona (2005).